Introduction to Neutron Scattering as a Tool for Characterizing Magnetic Materials

Cindi L. Dennis

Abstract This chapter will introduce the concepts of neutron scattering, including the benefits and limitations, especially in comparison to other experimental scattering techniques. It will also describe recent expansion of neutron scattering capabilities, including polarization analysis and time resolution, and their potential. Example applications demonstrating the power of neutron scattering as a characterization tool will be discussed.

Keywords Neutron scattering · Small angle neutron scattering · Neutron reflectivity · Neutron diffraction · Polarization analysis · Time resolution · Characterization · Magnetic materials

1 Introduction

Fundamentally, there are different ways to probe materials, including wavelength-specific electromagnetic radiation (e.g., visible light, infrared, x-rays, etc.) or particles (e.g., electrons and neutrons) or forces (e.g., electrostatic, electromagnetic, etc.), to name three common ones. These probes can then be used in diverse ways to determine different properties of a material, such as optical or force microscopy to image the surface of a material, electron or x-ray diffraction to learn about composition and atomic-level crystal structure, magnetometry to understand magnetic changes in a material, and light/x-ray/neutron scattering to learn about micro- and meso-scale structure as well as atomic structure. These measurements can be made as a function of applied magnetic field, temperature, stress or strain, etc., to better understand the behavior of a material, either fundamentally or for its specific application. Choosing the right technique to answer a specific question about a material is critical; understanding the potential and the limitations of a

C. L. Dennis (✉)
National Institute of Standards and Technology, Gaithersburg, MD, USA
e-mail: cindi.dennis@nist.gov

V. Franco, B. Dodrill (eds.), *Magnetic Measurement Techniques for Materials Characterization*, https://doi.org/10.1007/978-3-030-70443-8_13

given technique is crucial to making an informed choice. Many different techniques have been discussed in other chapters of this book. Here, the focus is on neutron scattering, specifically the elastic coherent techniques of neutron diffraction (ND), neutron reflectivity (NR), and small angle neutron scattering (SANS).

This chapter is not an exhaustive treatise on neutron scattering. The interested reader is referred to the following chapter and to a number of excellent references, either generally [1] and [2] and [3] or for specific techniques like polarization analysis [4, 5] or time resolution [6, 7]. Instead, this chapter will introduce the basic physics concepts, using a few limited equations for understanding experimental data. Then, specific instrumentation and measurement methods, including what to look for in the data, will be discussed with examples.

2 Neutron Sources

Unlike with electromagnetic radiation (e.g., visible light or x-rays) or electrons or forces, there are no easy lab-scale sources of neutrons. Instead, neutrons are generated though one of two sources: a steady neutron flux that is a by-product of controlled fission in a nuclear reactor, such as the split core reactor at the National Institute of Standards and Technology's (NIST) Center for Neutron Research [8], or pulses of neutrons from a spallation source, such as those generated from the impact of protons accelerated at a steel target filled with mercury as at the Spallation Neutron Source at Oak Ridge National Laboratories [9].

Neutron fluxes are typically higher at spallation sources than from reactors because all the neutrons in a pulse can be used. (The time of flight yields the velocity of the individual neutrons, which is necessary for the scattering wave vector Q to be determined, as explained below.) In contrast, neutrons from a reactor are a steady stream with a range of energies/velocities and therefore typically must be monochromated so that the velocity of the neutrons is known with reasonable uncertainty. This throws away a significant amount of intensity. In either case, the total flux is still significantly lower than an equivalent x-ray source.

The neutrons generated come in two "temperatures": thermal neutrons which have a very short wavelength (e.g., 2 Å, but it depends on the temperature of the moderator and/or monochromator that the neutrons pass through) and "cold" neutrons with longer wavelength (e.g., 7 Å, which result from passing thermal neutrons through a cold source composed of, for example, liquid hydrogen or solid deuterium oxide ("heavy water") to slow the neutrons down further). The difference in wavelength allows the neutrons to probe different length scales in materials. Reactors produce a larger flux of cold neutrons; spallation sources produce more thermal neutrons.

Although the Fukushima nuclear disaster in 2011 has reduced the ranks of power generation nuclear reactors globally, there are still a number of research reactors and spallation sources available around the world. A non-exhaustive list includes the NIST Center for Neutron Research (NCNR) and the Spallation Neutron Source

(SNS) and High Flux Isotope Reactor (HFIR) in the USA, the Open-Pool Australian Lightwater reactor (OPAL) in Australia, the Japan Proton Accelerator Research Complex (J-PARC) in Japan, ISIS Neutron and Muon Source in the UK, the Institut Laue-Langevin (ILL) in France, Forschungs-Neutronenquelle Heinz Maier-Leibnitz (FRM II) in Germany, and the (under construction as of 2020) European Spallation Source (ESS) in Sweden. All of these facilities have teams of instrument scientists who operate specific instruments (beamlines) at each location and host user scientists from around the world for specific experiments, awarded through beamtime proposals. More information about procedures for applying for beamtime can be found on each facility's website.

3 Physics of Neutron Scattering

The idea of scattering is straightforward. You direct a beam of something, electromagnetic radiation or particles, at the material of interest. The beam then interacts with the material that it passes through, causing the beam to deviate from a straight line. The physics can be simple or complicated, depending on the specific process causing the scattering and whether or not it is elastic or inelastic. To aid in understanding, we compare three specific types of beams and their interactions: x-rays, electrons, and neutrons (see Fig. 1).

X-rays scatter off the electrons surrounding the nucleus of an atom through an electromagnetic interaction. The more electrons there are, the more efficiently the x-ray is scattered (see Fig. 2). Therefore, if you have a material composed of heavy atoms (like yttrium and copper) and light atoms (oxygen and barium), the heavy atoms dominate the signal. As a result, if you are looking for the position of an oxygen atom in a high-temperature superconductor filled with heavy atoms of yttrium and copper, it will be challenging to see it.

Charged particles like electrons also interact with the electrons surrounding the nucleus, but through an electrostatic interaction. They are either attracted or repelled depending on the sign of the charge on the particle. As a result, electron transparent materials must be very thin (<100 nm) to avoid significant attenuation of the signal (see Fig. 2).

Neutrons, in contrast, interact with a material differently, for three reasons. First, the neutron has no charge. The neutrons interact with the material primarily through the nuclear force, which is very short range (as compared to the electrostatic/electromagnetic forces). As a result, most neutrons pass unattenuated through materials. This enables complex sample environments, since the neutrons will go through the container holding the sample readily. Unfortunately, the end result is that significantly more material is required and much longer counting times (as the flux of neutrons is not very high to begin with) in order to get good statistics for neutron scattering, as compared to the same x-ray/electron scattering technique. Second, neutrons have a magnetic moment. Therefore, neutrons can also interact with the material through dipole-dipole interactions if there are unpaired electrons in

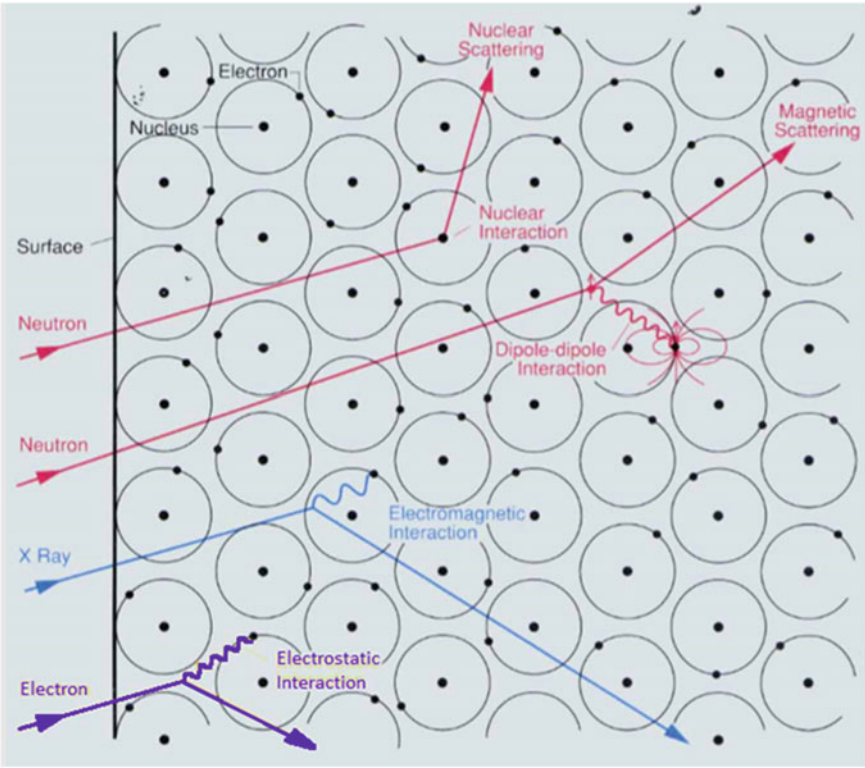

Fig. 1 Beams of neutrons, x-rays, and electrons interact with a material through different mechanisms. (Used with permission from [3]. Modified colors for better visibility)

the material. The end result is that neutrons can probe not only the nuclear structure of a material but also the magnetic structure.

Third, neutrons have a unique scattering cross section [10] which depends heavily upon isotope, as compared to x-ray and electrons, which have a more straightforward dependence of scattering on the atomic number. For example, hydrogen (H) has a small neutron scattering cross section of 1.7583 barns (1.7583×10^{-24} cm^2), but deuterium (D) is much larger at 5.592 barns. The end result is that neutrons are uniquely placed to study hydrogen-containing compounds, like polymers, something that x-rays and electrons do not see as well. In addition, the non-monotonic behavior of the penetration depth (see Fig. 2) of neutrons allows the use of "contrast matching" to pick and choose what is studied. This means that an isotopic substitution of elements, such as deuterium for hydrogen, can significantly change what is seen (see Fig. 3). A good example of this is in iron oxide magnetic nanoparticles dispersed in water. The nuclear scattering length density of magnetite is closely matched at 6.975×10^{-6}/Å^2 to that of "heavy water" D_2O at 6.335×10^{-6}/Å^2, but is significantly different from that of "light water" or H_2O

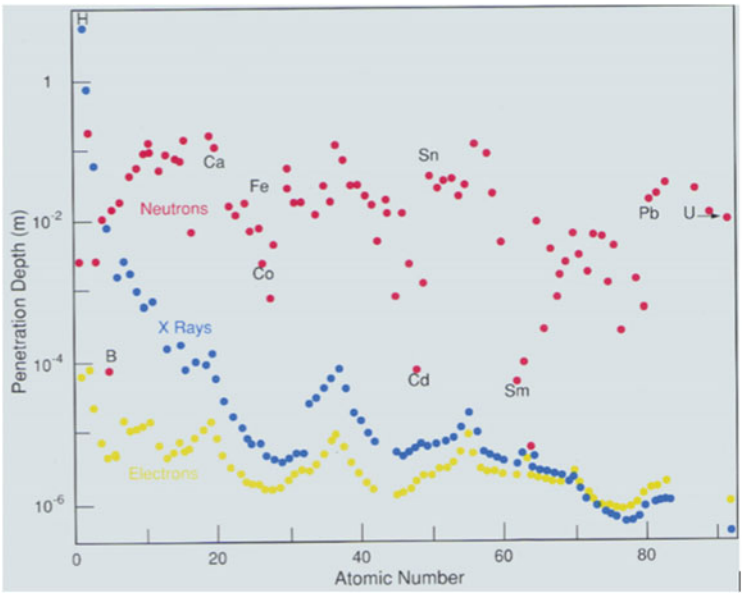

Fig. 2 Penetration depth of neutrons, electrons, and x-rays by element (Used with permission from [3])

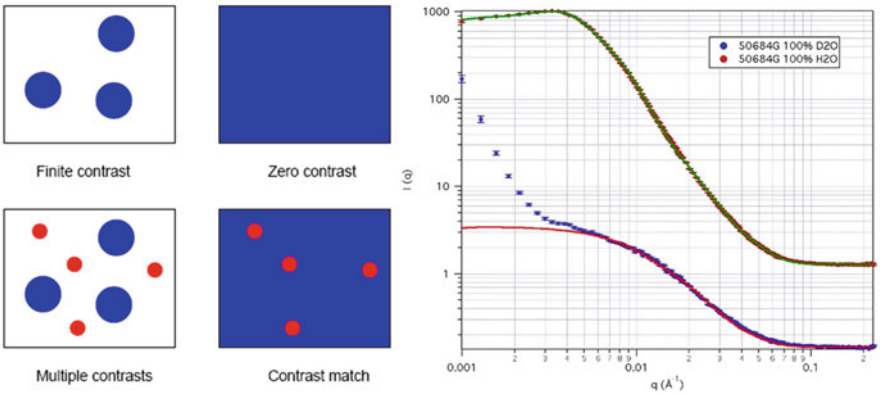

Fig. 3 (Left) Schematic of contrast matching for an iron oxide nanoparticle dispersed in water. (Right) SANS data showing nuclear and magnetic scattering of the iron oxide nanoparticles in light (H_2O) and heavy (D_2O) water

at $-0.561 \times 10^{-6}/\text{Å}^2$. As a result, changing the isotope of hydrogen in the water enables the user to make visible or invisible the nuclear scattering from the iron oxide. Therefore, the magnetic scattering can be determined, even though it is only 4% of the signal intensity (see Fig. 3).

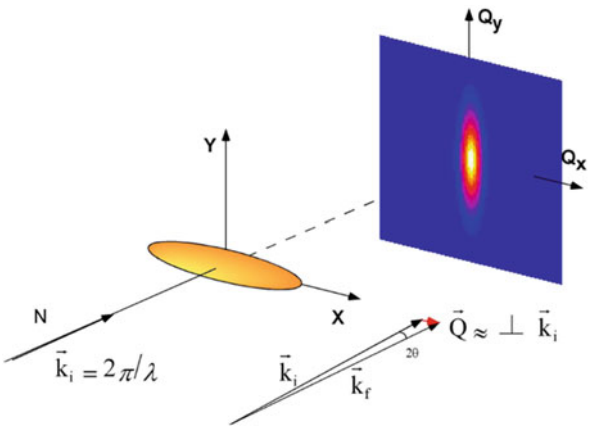

Fig. 4 Scattering schematic for SANS. (Courtesy of NCNR)

From quantum mechanics, we know that neutrons have wave-particle duality. This means we can associate a neutron wavelength λ with the velocity **v** of the neutron, through:

$$\frac{h\vec{k}}{2\pi} = m\vec{v} \tag{1}$$

where h is Planck's constant, **k** is the neutron wave vector ($k = 2\pi/\lambda$), and m is the mass of the neutron. Since the wavelength of the neutron is much larger than the range of the nuclear force, the nucleus acts as a point scatterer and scatters the neutrons isotropically. (This is not the case for x-rays, nor is it the case for dipole-dipole "magnetic" neutron scattering.) In all neutron scattering experiments, the result is the intensity I of neutrons scattered per incident neutron as a function of the momentum transfer ($h\mathbf{Q}/2\pi$) and energy transfer (ε):

$$\mathrm{I}(\mathbf{Q}, \varepsilon) = \mathrm{NF}(\mathbf{Q}, \varepsilon)\, \mathrm{S}(\mathbf{Q}, \varepsilon) \tag{2}$$

where N is the number of scatters per unit volume, $\mathbf{Q} = \mathbf{k_i} - \mathbf{k_f}$ and $\mathbf{k_i}$ is the incident wave vector and $\mathbf{k_f}$ is the scattered wave vector (see Fig. 4), and F(**Q**, ε) is the form factor and S(**Q**, ε) is the structure factor. (These "factors" will be briefly discussed later.) Interestingly, the anisotropy inherent in magnetic scattering manifests itself as a simple rule: magnetic scattering can only be seen when the scattering vector **Q** is perpendicular to the magnetic field of an unpaired electron or, more generally, the sample magnetization. With this equation, there are three types of scattering:

1. Elastic coherent scattering ($\varepsilon = 0$).
2. Inelastic coherent scattering ($\varepsilon \neq 0$).[1]

[1] A triple-axis spectrometer (at a reactor) and a chopper spectrometer (at a spallation source) are examples of techniques which provide information about the collective motions of atoms (e.g., phonons or magnons) as not only **k** and **k'** must be determined to get **Q** but also ε.

3. Incoherent scattering.

Only elastic coherent scattering will be discussed here, of which ND, NR, and SANS are example techniques. They provide information about the equilibrium structure.

One final comment: there exist multiple neutron scattering instruments which make similar measurements, as they are tailored specifically to the science they are designed to study because there is always a trade-off between intensity and resolution. For example, SANS (see Fig. 4) has a small diffraction angle for studying large objects, but also a reduction in monochromatization—only enough to match the angular resolution to maximize neutron flux. In contrast, back scattering has very good energy resolution, but uses large analyzer crystals so it has poor Q resolution.

4 Neutron Diffraction

Neutron diffraction (see Fig. 5) is analogous to x-ray diffraction and follows Bragg's law:

$$n\lambda = 2dsin\,(\theta) \tag{3}$$

where 2θ is the scattering angle, d is the lattice constant, and n is an integer. λ, the wavelength of the probe, is typically chosen to be on the order of the lattice spacing. Therefore, I(Q) is typically dominated by S(Q) where S(Q) is the structure factor and is primarily dependent upon the placement of the specific atoms. Diffraction provides information about the dimensions of the crystal lattice and the positions of atoms within it, the symmetry of the crystal, and the extent of thermal vibrations in various directions. It is a very useful tool for studying stress and strain as well as texture in materials. However, unlike x-ray diffraction, the magnetic moment of the neutron means that it is possible to see magnetic lattices as well as atomic lattices. The atomic and magnetic scattering can be separated, for example, by changing the orientation of a saturating magnetic field from parallel to perpendicular to Q. When H and Q are parallel, only nuclear scattering is seen. When H and Q are perpendicular, the magnetic scattering is added to the nuclear scattering, changing the peak intensities. For example, when measuring a ferromagnet such as MnPtGa (see Fig. 6), the atomic lattice spacing between the Mn atoms and the magnetic lattice spacing between the Mn atoms is the same, since the Mn moment is parallel to its neighbor. When decreasing the temperature so that MnPtGa changes to a canted anti-ferromagnet, the atomic lattice spacing between the Mn atoms is double that of the magnetic lattice spacing, since the Mn atoms are coupled anti-ferromagnetically (see Fig. 6). (Recall: doubling the lattice spacing gives rise to a peak at the half order position.) The latter is an alternative approach to changing the magnetic field orientation. Therefore, neutron diffraction also enables a direct probe of the magnetic structure and has been particularly useful for anti-ferromagnetic and spin-canted materials.

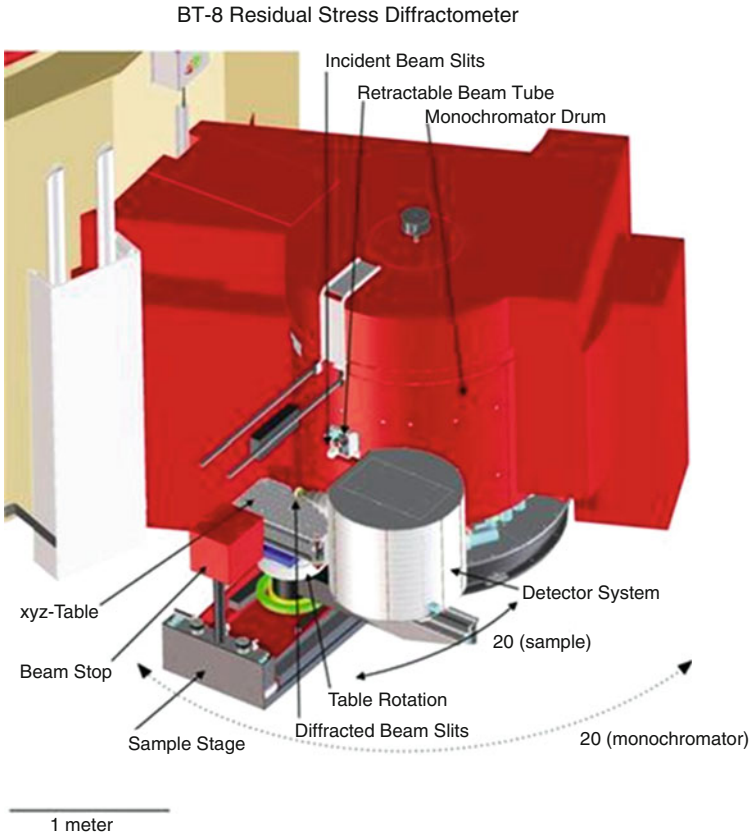

Fig. 5 Schematic of a neutron diffractometer. (Courtesy of NCNR)

5 Neutron Reflectivity

Neutron reflectivity is analogous to x-ray reflectivity (see Fig. 7), where x-rays/neutrons are reflected off a smooth surface at very small angles to study the surface structure. For light, this works only for very smooth surfaces at the top and follows Fresnel's law. For neutrons, the "surface" will actually be all interfaces within a few thousand nanometers of the topmost layer. This makes neutron reflectivity a very powerful method for probing interfaces, especially buried interfaces. As most modern devices have shrunk in size and have at least one interface, if only from a protective coating, there are many avenues for research here. For example, a recent review summarized the studies on the self-assembly process of magnetic nanoparticles on a surface and the impact of the surfactant, surface preparation, and applied magnetic field (see Fig. 8).

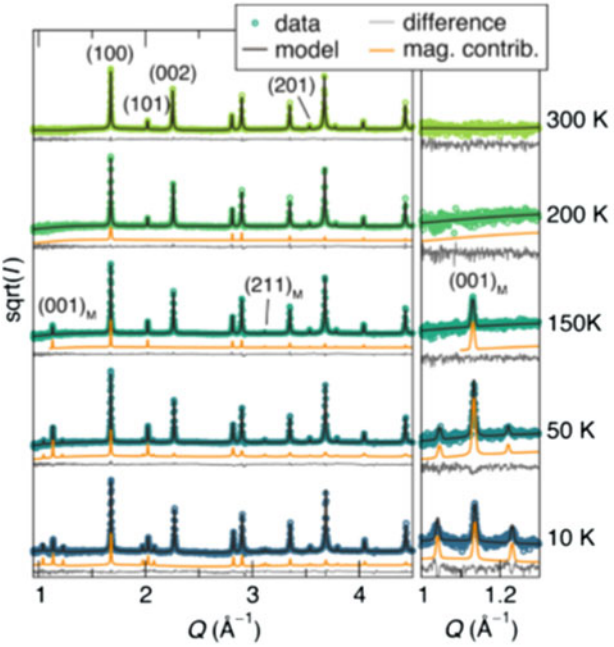

Fig. 6 Experimental ND data demonstrating the transition of MnPtGa from a ferromagnet, to a canted anti-ferromagnet, to the eventual formation of a spin-density-wave state at low temperatures. (Used with permission from [11])

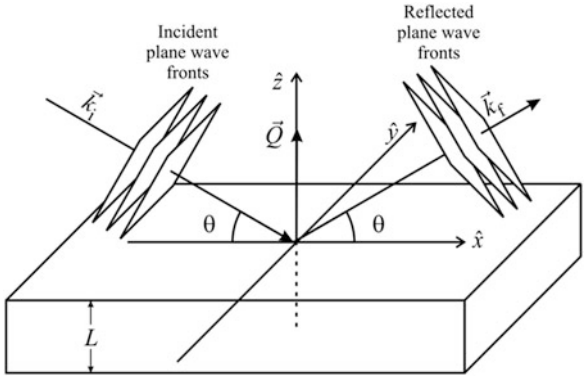

Fig. 7 Schematic of a neutron reflectometer (Courtesy of NCNR)

When examining NR data, the spacing of the oscillations and/or peaks and the height and shape of these features are indicative of the layer thickness and the interface quality. Generally, the less dampening of the oscillations there is, the cleaner the interface is; the closer the oscillations are in Q, the thinner the layers are in practice.

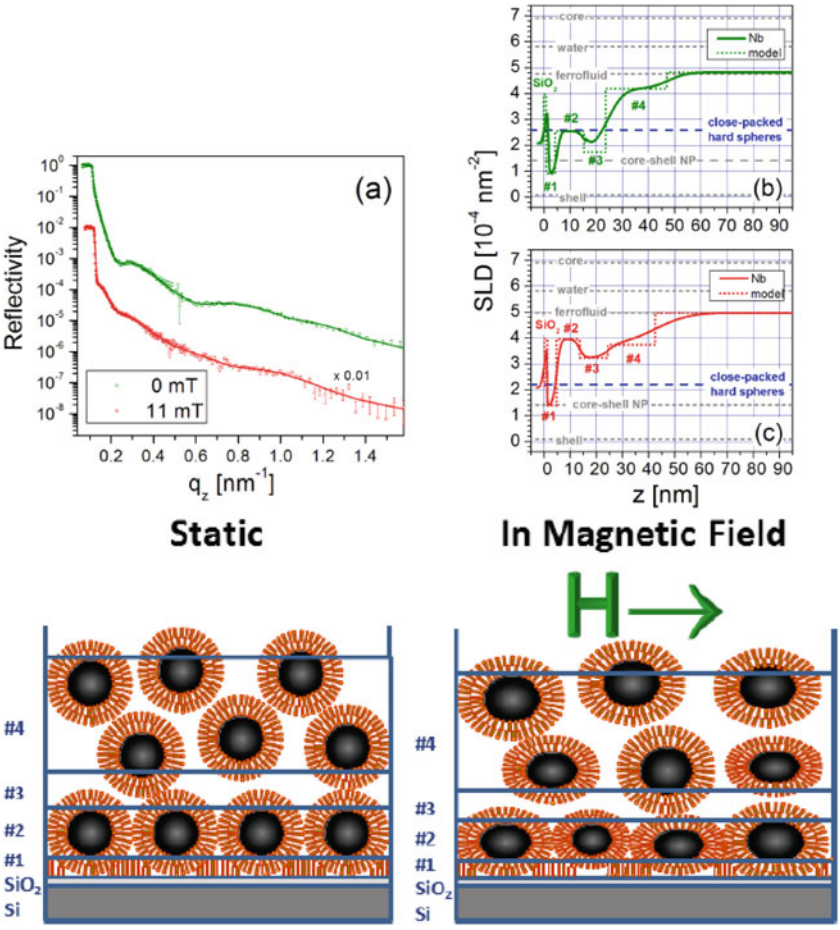

Fig. 8 (Top) (**a**) NR data on iron oxide nanoparticles coated with oleic acid and their self-assembly onto a Si/SiO_2 surface as a function of applied magnetic field. The nuclear scattering length density profiles as a function of distance z from the Si surface at applied magnetic fields of (**b**) 0 mT and (**c**) 11 mT, obtained from the model fits of the NR data in (**a**). (Bottom) Model showing hexagonal close packed structure in the initial layer followed by increasing disorder in the layers above. The magnetic field increases the disorder and elongation in the field direction. (Used with permission from [12])

6 Small Angle Neutron Scattering

Small angle neutron scattering also obeys Bragg's law (Eq. 3), but now the size d is that of larger objects, such as pores in rock or nanoparticles in solution or blocks in a co-polymer. Therefore, longer wavelengths are needed and/or smaller angles. Then,

I(Q) is typically dominated by F(Q) where F(Q) is the form factor and is dependent mainly upon the shape of the object. Whereas ND provides information about the atomic structure, SANS provides information about the shape and size of nanoscale to microscale structure.

Within SANS, there are specific instruments that cover specific dimensions (see Fig. 9 for examples from NCNR). 30 m SANS covers dimensions approximately 1–700 nm, ultra-SANS (USANS) covers approximately 100–20,000 nm, and very-SANS (VSANS) covers approximately 1–2000 nm.

Data reduction [13] and data modeling programs [14] are readily available and account for differences in data formatting between instruments at different facilities. Data reduction takes into account the total flux of neutrons incident on the sample (by removing the sample, so that the beam is "open"), what the background is for the instrument configuration (by a blocked beam), and what the transmission of the sample is (by measuring the central beam intensity at the detector). The scattering measurement blocks the main transmitted beam so that the scattered intensity can be measured. While data are collected on a 2D detector, they are rarely analyzed that way. Instead, the data are averaged (see Fig. 10). This could be a circular average where only the radius from the center matters. It could be a sector average, if there is anisotropy in the data such as shown in Fig. 10, for example, due to an applied magnetic field or structural anisotropy such as chaining. Finally, it could be an annular average, where the data at a specific radius are plotted as a function of angle.

Interpretation of SANS data requires specific models, and the details of the model matter greatly. Therefore, secondary information is always necessary in order to make good guesses about what model and parameters to use. For example, the same dataset (see Fig. 11) can be modeled with a polydisperse sphere or with a parallelepiped. The shapes are quite different, and to most experimentalists, the fits are equally good. However, the exact detail of the transition to background is quite different between the two models and is significant to the interpretation.

However, in looking at SANS data, you are looking for the location in Q of peaks or turn-overs or asymmetry in the data. For example, the turn-overs in Fig. 12 of modeled polydisperse spheres are located at different Q values (where $Q \approx 2\pi/d$), which are indicative of the differing size of the objects; in this case, the size is a diameter. The difference in intensity is less important, as the total intensity is spread out over the whole Q range, including low Q values not accessible for the specific instrument. In addition, when looking at SANS data, recall that the selection rules dictate that the magnetic scattering only appears when the sample magnetization is perpendicular to Q. Therefore, magnetic scattering has a characteristic sinusoidal-like pattern, as seen in Fig. 10.

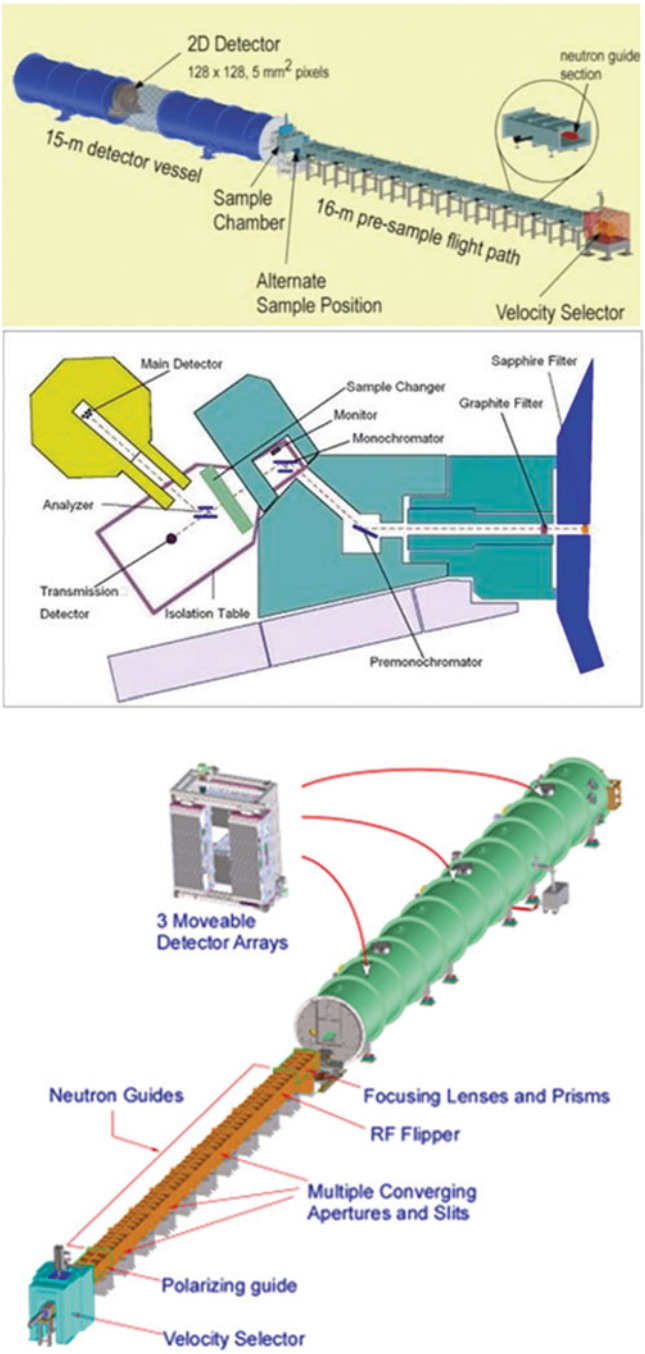

Fig. 9 (Top) SANS instrument schematic. (Middle) USANS instrument schematic. (Bottom) VSANS instrument schematic. (Courtesy of NCNR)

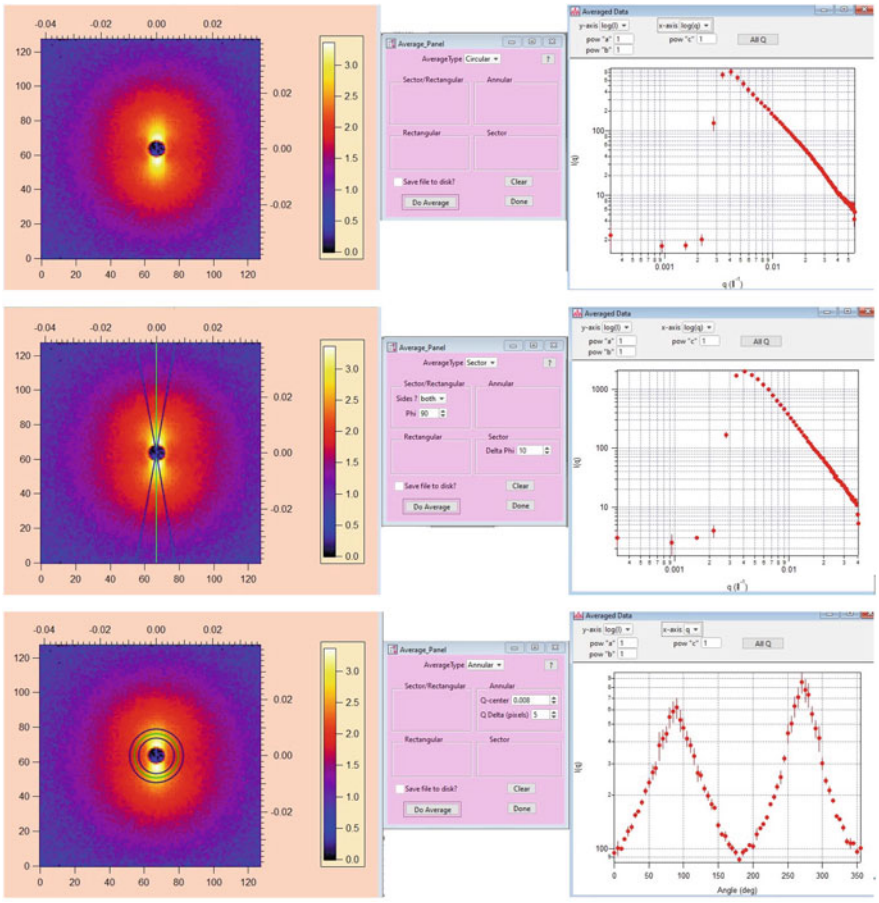

Fig. 10 Image of 2D detector data collected on iron oxide nanoparticles in water with (top) circular averaged I(Q), (middle) sector averaged I(Q), and (bottom) annular averaged I(Q)

7 Polarization Analysis

Normally, the neutron source is unpolarized, so the neutron moments point in all directions. However, very interesting physics can be done if the neutron moments have a large degree of alignment or polarization. (Polarization analysis can occur using any of the scattering techniques, but it is only discussed here for SANS and NR, see Fig. 13, due to space constraints. The basic principles apply for all methods.) While this polarization can originate from a large magnetic field applied

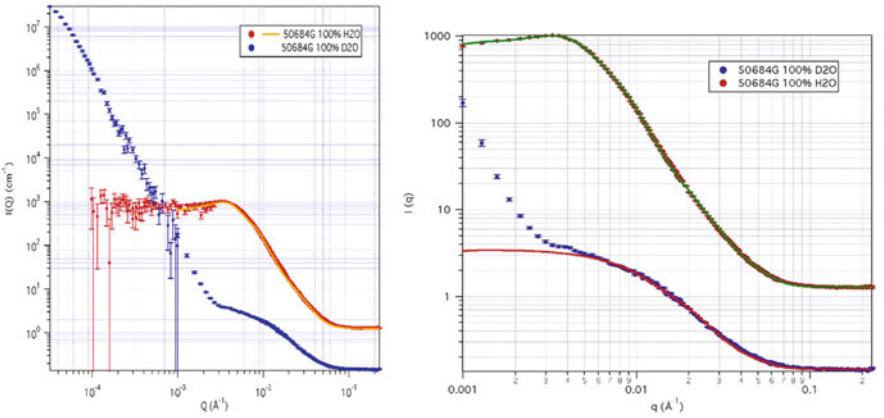

Fig. 11 Iron oxide nanoparticles in water, fit with a (left) spherical model and (right) parallelepiped model. Note the difference in the shape of the transition to background of the two models

Fig. 12 Model SANS data of spheres of different radii

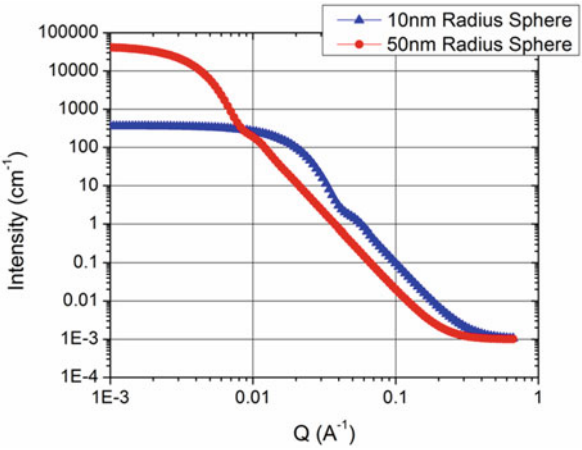

to the neutron beam, in practice, a polarizing device is used.[2] For example, a supermirror (e.g., alternating layers of Fe and Si which reflect away the undesired spin state), or a helium-3 spin filter (which adsorbs the undesired spin state), or a Heusler crystal (which has a scattering length of zero for the undesired spin state) is placed in the beam (see Fig. 9). This polarization is then maintained via a small guide magnetic field (on the order of 1 mT).

Experimentally, once you have a polarized beam, the neutrons are labeled as spin up (parallel to the guide field) or spin down (antiparallel to the guide field). When the polarized neutrons interact with a material, their spin direction can change.

[2]At NCNR, the incident polarization on the two SANS instruments is done with a V-shaped supermirror cavity.

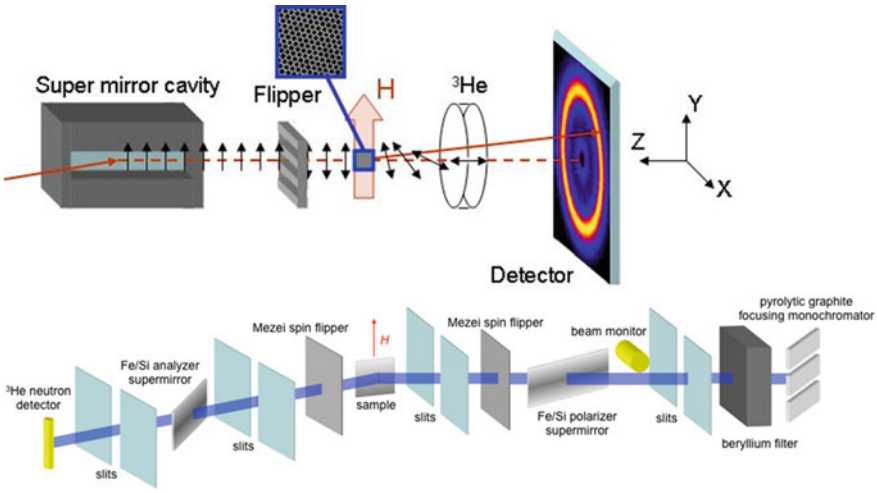

Fig. 13 (Top) Schematic of SANS including polarization of the neutron beam. (Bottom) Schematic of NR including polarization of the neutron beam (Courtesy of NCNR)

For magnetic materials, the non-spin flip scattering (spin-up to spin-up scattering and spin-down to spin-down scattering) represents nuclear scattering; the spin flip scattering (spin-up to spin-down scattering and spin-down to spin-up scattering) represents magnetic scattering only. The components of the magnetization parallel and perpendicular to the applied magnetic field can be separated when the polarization is perpendicular to the scattering wave vector, and the vector magnetization within the material can be unambiguously determined.

The next step is to be able to flip the neutron polarization at will, to create spin-up and spin-down configurations. A flipper is used to change the direction of the moment of the neutron relative to the guide field. This is typically done by having a coil of wire to cancel the guide field and a second coil to create a field perpendicular to reverse the moment of the neutron. (While this is actually a quantum mechanical effect, like many things in magnetism, a simple classical analogue works: the perpendicular field causes a torque to act on the neutron and rotate it.) After the polarized beam passes through the material, the polarization of the neutron beam must be determined. This is often done in SANS with polarized helium-3 cells, in which neutrons of one spin state are absorbed, while neutrons with the opposite orientation travel through relatively unimpeded [15].

Data reduction of polarized neutrons is more complicated than the unpolarized data [15]. Additional corrections include the efficiency of the polarizers (supermirror and/or He-3 cell) and, if appropriate, the decay of the He-3 cell polarization as a function of time. Polarization analysis permits the unique determination of the magnetization vector within a sample. This has already demonstrated enormous utility for determining the vector magnetization when studying magnetic nanoparticles and thin films. At low fields, it has shown the internal magnetic domain structure (see Fig. 14), enabling correlation of the magnetic domains with

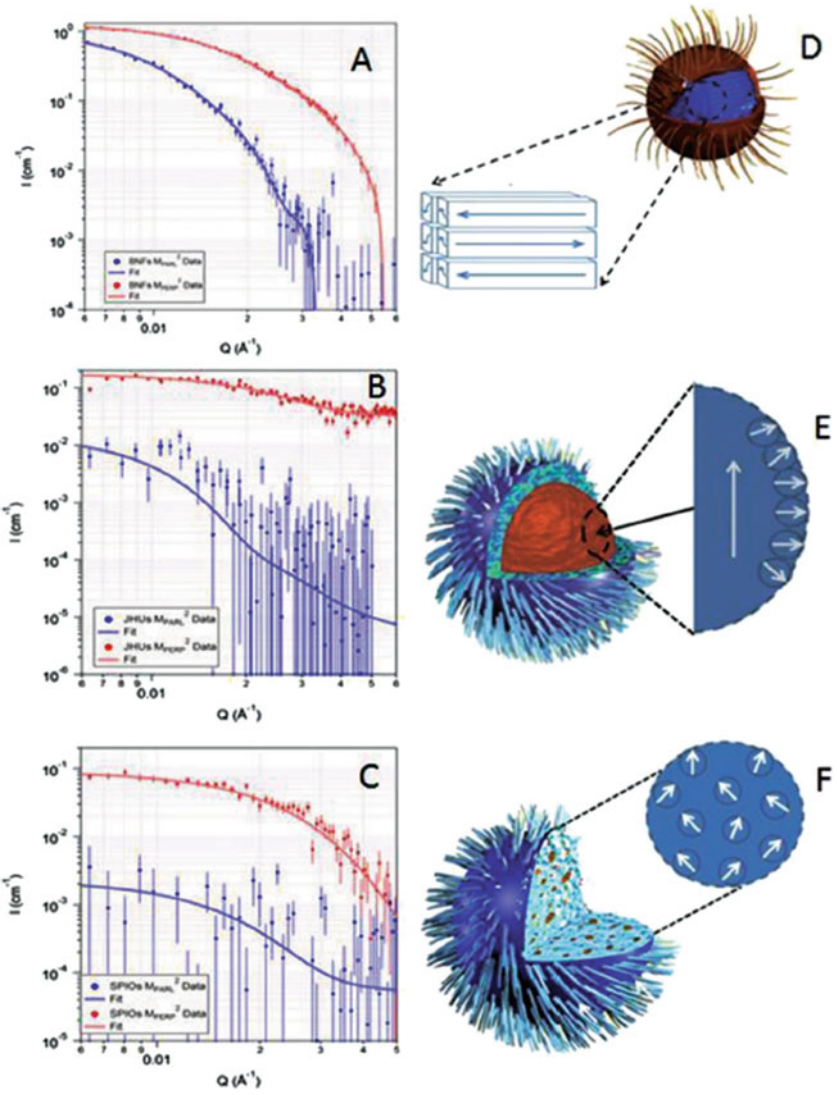

Fig. 14 Internal magnetic domain in iron oxide nanoparticles as determined with polarization analysis in SANS. (**a**), (**b**), and (**c**) show the parallel and perpendicular magnetic scattering and their fits for three different iron oxide nanoparticles while (**d**), (**e**), and (**f**) are schematics of the domain structure from (**a**), (**b**), and (**c**) respectively. (Used with permission from [16])

the AC field response and therefore the heat generation for the cancer treatment hyperthermia [16]. It has also been used to demonstrate surface spin canting in compositionally and structurally uniform magnetic nanoparticles under a nominally saturating magnetic field (see Fig. 15) and how the surface spins change as a function of applied magnetic field and temperature [17].

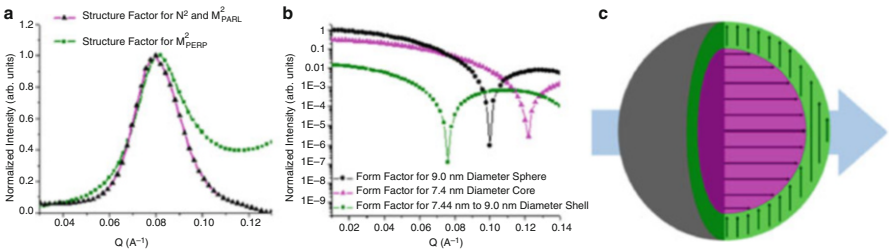

Fig. 15 Surface spin canting on iron oxide nanoparticles as determined with polarization analysis in SANS. (**a**) is the structure factor and (**b**) is the form factor for the nuclear and magnetic (parallel and perpendicular) scattering. (**c**) is a schematic of the magnetic structure within the iron oxide nanoparticle based on (**a**) and (**b**). (Used with permission from [17])

Early studies (see Fig. 16) of bilayers of Fe/Gd thin films demonstrated the power of polarized NR, as they were able to identify the antiferromagnetic coupling between the layers and demonstrate the diverse range of magnetic orientations that resulted as a function of layer thickness and temperature.

8 Time Resolution

This is naturally done at a spallation source, where all the neutrons are time stamped in order to determine their energies. It is also possible to time stamp neutrons from a reactor. This leads to two forms of time resolution: time-of-flight (TOF) and time-resolved (TR). TOF is limited by the spread of the neutron beam as it travels, resulting in overlap of different time signals, thereby determining the size of the bins. Time-resolved puts a chopper in the beam (see Fig. 17), breaking up the neutron flux into small packets. These can then be time synchronized to something else, like an oscillating electric or magnetic field or sinusoidal stress. The neutrons can then be binned according to when they interacted with the sample with respect to the AC stimulation, permitting tracking of the time-dependent response. TR is limited by the spread of the beam packet (due to having a polychromatic beam even after monochromating) during flight from the sample to the detector as well as detector electronics. Another limitation is that the chopper throws away neutrons, further reducing your signal. Early work has confirmed expected behavior in magnetic nanoparticles (see Fig. 18).

9 Summary

In summary, neutrons are a unique and powerful tool with which to characterize materials. Advantages included *in situ* measurements and the ability to highlight

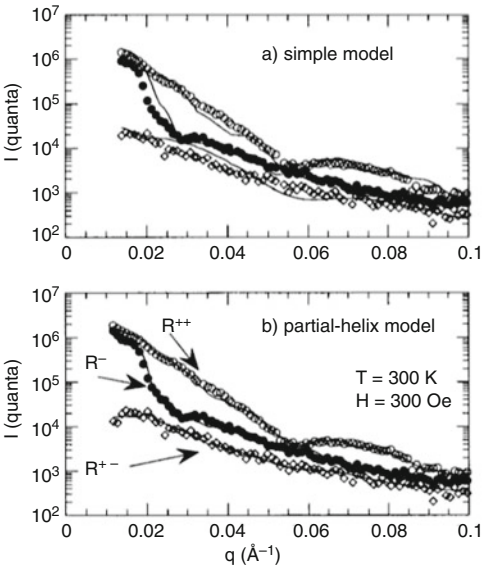

Fig. 16 Experimental polarized NR data on Fe/Gd, demonstrating the formation of spin canted states in the Gd. (Used with permission from [18])

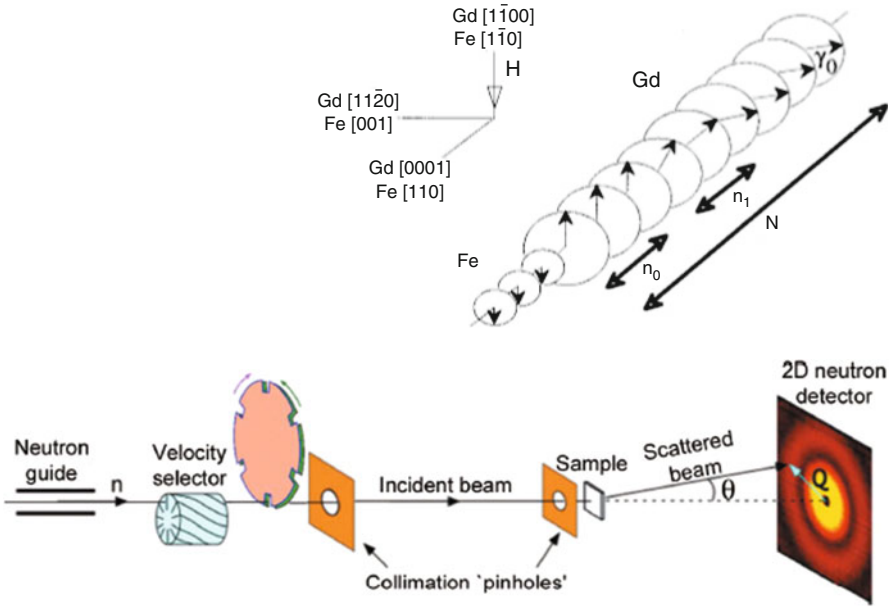

Fig. 17 Time-resolved SANS instrument schematic (Used with permission from [7])

different aspects of the sample with contrast matching. Furthermore, neutrons also have exquisite sensitivity to the vector magnetization on the nanoscale. However, although access is readily available via user proposal system, neutrons do require specialized facilities. Therefore, if it is possible to measure the same property with

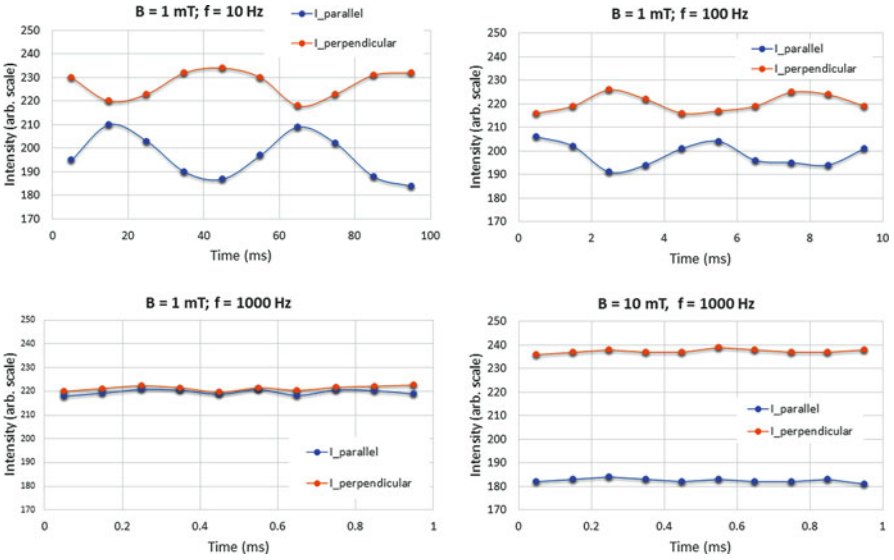

Fig. 18 TOF data on magnetic nanoparticles showing reversal behavior at low frequencies, and then blocked behavior at low fields and high frequencies, before reversal behavior reappears at high fields and high frequencies. (Used with permission from [19])

a lab-scale technique, that is preferable (especially as neutron experiments often require more material and longer counting times than other scattering methods). However, there are a number of cases where neutrons are the best method available, such as vector magnetization of an ensemble of nanoparticles or magnetization reversal mechanisms in magnetic thin films, to name just two. This then opens up new avenues of research and new insights into materials.

Acknowledgments C.L.D. thanks Julie Borchers, Kathryn Krycka, Andrew Jackson, William Ratcliffe, Markus Bleuel, Charlie Glinka, John Barker, Steve Kline, and Paul Butler for many useful discussions over the years.

References

1. T. Chatterji, *Neutron Scattering from Magnetic Materials* (Elsevier, New York, 2006)
2. B. Hammouda, *Probing Nanoscale Structures – The SANS Toolbox* (NIST, Gaithersburg, MD, 2016)
3. R. Pynn, *Neutron Scattering: A Primer* (Los Alamos Neutron Science Center)
4. K.L. Krycka, J.A. Borchers, Y. Ijiri, R. Booth, S.A. Majetich, Polarization-analyzed small-angle neutron scattering. II. Mathematical angular analysis. J. Appl. Crystallogr. **45**, 554–565 (2012)
5. A. Michels, J. Weissmueller, Magnetic-field-dependent small-angle neutron scattering on random anisotropy ferromagnets. Rep. Prog. Phys. **71**, 066501 (2008)

6. A. Wiedenmann, U. Keiderling, K. Habicht, M. Russina, R. Gaehler, Dynamics of field-induced ordering in magnetic colloids studied by new time-resolved small-angle neutron-scattering techniques. Phys. Rev. Lett. **97**, 057202 (2006)
7. C. Glinka, M. Bleuel, P. Tsai, D. Zakutna, D. Honecker, D. Dresen, F. Mees, S. Disch, Sub-millisecond time-resolved small-angle neutron scattering measurements at NIST. J. Appl. Crystallogr. **53**, 598–604 (2020)
8. J. Rush and R. Cappelletti, The NIST Center for Neutron Research: Over 40 years serving NIST/NBS and the nation, NIST Special Publication 1120 (2011)
9. "How SNS Works," 2020. [Online]. Available: https://neutrons.ornl.gov/content/how-sns-works
10. V.F. Sears, Neutron scattering lengths and cross sections. Neutron News **3**(3), 29–37 (1992)
11. J. Cooley, J. Bocarsly, E. Schueller, E. Levin, E. Rodriguez, A. Huq, S. Lapidus, S. Wilson, R. Seshadri, Evolution of noncollinear magnetism in magnetocaloric MnPtGa. Phys. Rev. Mater. **4**, 044405 (2020)
12. K. Theis-Bröhl, A. Saini, M. Wolff, J. Dura, B. Maranville, J. Borchers, Self-assembly of magnetic nanoparticles in Ferrofluids on different templates investigated by neutron reflectometry. Nano materials **10**, 1231 (2020)
13. S. Kline, Reduction and analysis of SANS and USANS data using IGOR pro. J. Appl. Crystallogr. **39**, 895–900 (2006)
14. "SASVIEW," 2020. [Online]. http://www.sasview.org/
15. K. Krycka, W. Chen, J. Borchers, B. Maranville, S. Watson, Polarization-analyzed small-angle neutron scattering. I. Polarized data reduction using Pol-Corr. J. Appl. Crystallogr. **45**, 546–553 (2012)
16. C. Dennis, K. Krycka, J. Borchers, R. Desautels, J. van Lierop, N. Huls, A. Jackson, C. Gruettner, R. Ivkov, Internal magnetic structure of nanoparticles dominates time-dependent relaxation processes in a magnetic field. Adv. Funct. Mater. **25**, 4300–4311 (2015)
17. K. Krycka, R. Booth, C. Hogg, Y. Ijiri, J. Borchers, W. Chen, S. Watson, M. Laver, T. Gentile, L. Dedon, S. Harris, J. Rhyne, S. Majetich, Core-Shell magnetic morphology of structurally uniform magnetite nanoparticles. Phys. Rev. Lett. **104**, 207203 (2010)
18. O. McGrath, N. Ryzhanova, C. Lacroix, D. Givord, C. Fermon, C. Miramond, G. Saux, S. Young, A. Vedyayev, Observation and interpretation of a partial Gd twisted spin state in an epitaxial Gd/Fe bilayer. Phys. Rev. B **54**, 6088 (1996)
19. C. Dennis, C. Glinka, J. Borchers, C. Grüttner, R. Ivkov, Effect of applied AC magnetic field on response of magnetic nanoparticles. J. Appl. Phys.. submitted